RSC Advances

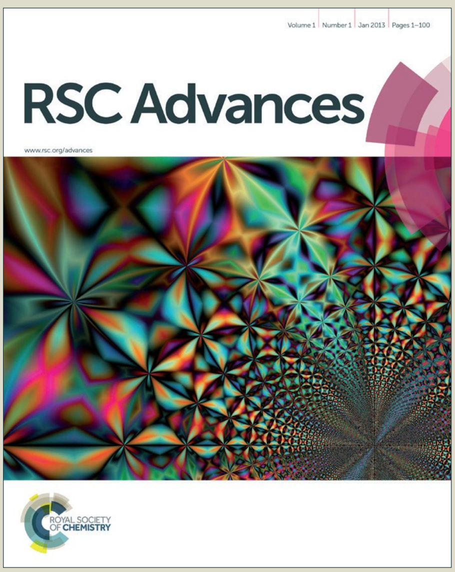

In this manuscript, the glutathione capped Au-nanoclusters showed a unique optical performance compared with their homological AuNPs with larger size. The luminescent intensity of the AuNCs could be enhanced due to the formation of aggregates. The AuNCs were then employed as a visual probe for the detection of Pb^{2+}, The method showed good linear response and selectivity, and the successful on-site detection of Pb^{2+} in lake water suggested its application potential.

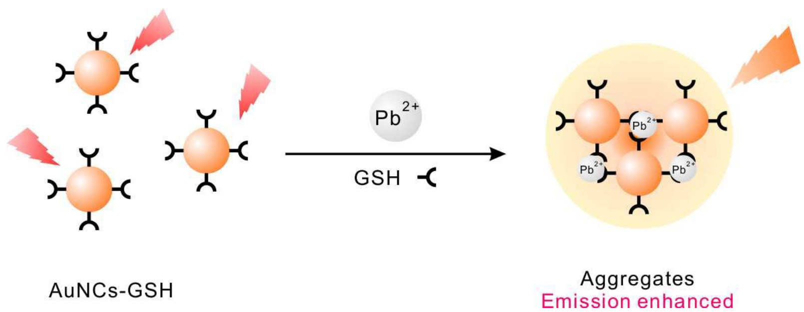

RSC Advances RSCPublishing

ARTICLE

Label-free detection of Pb^{2+} based on aggregation-induced emission enhancement of Au-nanoclusters

Cite this: DOI: 10.1039/x0xx00000x

Received 00th January 2012,
Accepted 00th January 2012

DOI: 10.1039/x0xx00000x

www.rsc.org/

Liya Ji,[a,b†] Yahui Guo,[b,c†] Shanni Hong,[b] Zhili Wang,[b] Kewei Wang,[b] Xing Chen,[b] Jianye Zhang,[a] Jiming Hu[c]* and Renjun Pei[b]*

Interestingly, the glutathione capped Au-nanoclusters presented here showed a unique optical performance compared with their homological AuNPs with larger size. The luminescent intensity of the AuNCs could be enhanced due to the formation of aggregation. The AuNCs were then employed as a visual probe for the detection of Pb^{2+} based on the aggregation-induce emission enhancement (AIEE) property of AuNCs. When the luminous glutathione capped AuNCs probes were encountered to Pb^{2+} ions, they rapidly formed aggregates through GSH-Pb^{2+} interaction in 1 minute, resulting in an enhanced luminescent intensity. The enhanced luminescent intensities showed a linear dependence on the concentrations of Pb^{2+} with satisfying selectivity towards 12 kinds of divalent metal ions. More importantly, the probe can also be used for on-site testing to inspect Pb^{2+} contamination by using a portable UV flashlight.

Introduction

Lead, with high economic value, is vastly produced (10.5 million tons, 2012) mainly for lead batteries for vehicles, energy storage and also for radiation shielding in healthcare industry, laboratories and nuclear installations.[1] There come accompanying concerns that how to work with lead safely and how to avoid and detect the lead contamination in work place and environment, since lead is a cumulative toxicant that poses significant health hazards on human, especially causing intellectual disabilities on children.[2] Lead exposure is even worse in many developing countries due to the low lead recovery in these countries. Therefore, an on-site, simple, low-cost and fast method is demanded in many occasions for the detections of Pb^{2+}.

The development of approaches to detect Pb^{2+} is of considerable significance and has become an important subject in analytical chemistry. Atomic absorption spectrometry, inductively coupled plasma mass spectroscopy, and inductively coupled plasma atomic emission spectrometry, have been developed for the detection of Pb^{2+}.[3-5] However, those methods necessitate the use of costly apparatus and are usually complicated, time-consuming and costly. Heavy metal ions detections by employing gold nanoparticles have showed excellent analytical performance due to the strong localized surface plasmon resonance and the colorimetric assays have attracted considerable attentions.[6-9] But the nanoparticles need further surface modifications, and are more susceptible to solution circumstance and could not reserve for long time. Though biosensors based on DNAzyme showed good selectivity and low detection limit, their practical use have been limited due to high cost, complicated processing and unstable RNA molecules.[10-13]

The emerging development and innovation of noble metal nanoclusters (NCs) with unique properties are at the leading edge of the rapidly developing field of nanotechnology, and have attracted increasing interest in recent years.[14,15] Due to their small size, the nanoclusters possess discrete electronic energy levels, display molecule-like distinct, optical absorption and emission characteristics,[16-20] and exhibit interesting catalytic activities. For example, the NCs could be used as selective catalysts for aerobic oxidations in water[21], or as hybrid oxygen electrocatalysts for nonaqueous lithium−oxygen batteries[22]. Especially those NCs made of gold and silver, presenting high quantum yields, excellent photostability, low toxicity and good biocompatibility, have attracted great interest in their biomedical applications and environmental monitoring.[23-25] Zhang et al. employed biocompatible GSH-AuNC as a new kind of radiosensitizer with good tumour deposition in body.[26] The GSH-AuNC showed a significant sensitization efficacy and has a high renal clearance due to its ultrasmall size. Xie et al. developed an optical label-free approach for the quick detection of Hg^{2+} by using a protein-capped AuNCs.[27,28] Durgadas et al. reported the use of fluorescent gold nanoclusters synthesized using bovine serum albumin for the sensing of copper ions in live cells.[29]

The interaction-responsive emission enhancement materials are ideal candidates in fluorescent biomedical detections with the advantage of low-background. Materials such as G-quadruplex specific dyes,[30-33] materials with aggregation-induced emission (AIE) property including multiple aromatic dyes[34-36] and fluorescent polymer[37-39] have attracted considerable interests and have been employed vastly in analytical chemistry and biomedicine applications. Relative to larger Au-nanoparticles, whose absorption bands depend on their size (or aggregation),[40,41] we found an intriguing phenomenon that the molecule-scale glutathione capped AuNCs rapidly formed aggregates through GSH-Pb^{2+} interaction, resulting in the aggregation-induced emission enhancement (AIEE). Based on the unique AIEE property of Au-GSH nanoclusters, a facile method was developed for the sensitive and selective detection of Pb^{2+}.

Experimental

Materials

Hydrogen tetrachloroaurate trihydrate ($HAuCl_4$•$3H_2O$) and L-Glutathione (GSH) were purchased from Sinopharm Chemical Reagent Co., Ltd. (Shanghai, China). All other chemical reagents were of analytical reagent grade and used without further purification. Measurements were performed in Tris-HCl (10 mM, pH 7.5) working buffer. All solutions were prepared with water purified by a Milli-Q system (Millipore, Bedford, MA, USA).

Instruments

Absorption spectra were recorded on a UV/Vis spectrometer (Lambda 25, PerkinElmer, USA) with Milli-Q water as the reference solution. Photoexcitation and emission spectra were recorded using a fluorescence spectrometer (F-4600, Hitachi Co. Ltd., Japan) with a Xenon lamp as excitation source, slit widths for the excitation and emission were set at 10 and 10 nm respectively. Transmission electron microscopy images of synthesized NCs were taken on a FEI Tecnai/G-20 microscope with accelerating voltage of 200KV. Digital photographs were taken by a digital camera (Canon PowerShot SX240 HS).

Synthesis of GSH-AuNCs

The GSH-AuNCs were synthesized according to the pervious literature.[42] 0.68 mL aqueous solutions of $HAuCl_4$ (1%) and 0.3 mL GSH (100 mM) mixed with 9.02 mL of ultrapure water under gentle stirring at 25°C for 5 min, the reaction mixture was then heated to 70°C and allowed to react for 24 h. The aqueous solution of GSH-AuNCs was then transferred to a dialysis tubing cellulose membrane with molecular weight cut-offs (MWCO) of 7 kDa (Solarbio Science & Technology Co., Ltd, Beijing) to remove the free GSH molecules. The solution of GSH-AuNCs was stored at 4 °C before use.

Measurement

The dialyzed GSH-AuNCs solution was diluted for 10 times with working buffer before using. Different concentrations of Pb^{2+} were prepared by diluting 0.1 M $Pb(NO_3)_2$ with working buffer. For Pb^{2+} detection, different concentrations of Pb^{2+} were mixed with 10 μL 10-fold diluted AuNCs, and the mixtures were adjusted to a final volume of 100 μL by adding different volumes of working buffer. After mixing and incubating at room temperature for 10 min, the luminescent spectra were recorded on a fluorescence spectrometer. The selectivity of the sensing system toward Pb^{2+} (50 μM) was evaluated by detecting cations including Mg^{2+}, Ca^{2+}, Mn^{2+}, Fe^{2+}, Co^{2+}, Ni^{2+}, Cu^{2+}, Zn^{2+}, Cd^{2+}, Ba^{2+}, Hg^{2+}, Pb^{2+}.

Real sample analysis

The lake water sample was obtained from Dushu Lake in Suzhou and used after filtration with a 0.45 μM membrane filter. The concentration of sample from lake water was determined by an Inductive Coupled Plasma Atomic Emission Spectrometer (PerkinElmer, Optima 8000). The lake water samples with various concentrations of Pb^{2+} were added to our detecting system, and the fluorescence spectra were recorded following the same process.

Results and discussion

AIEE Property of AuNCs

The thiolate-capped NCs are formed through the reduction of Au(I)-thiolate complexes, which generated from the reaction between Au(III) salts and thiols. The synthesis course included a kinetically controlled reduction process and a thermodynamically controlled size-focusing process.[25,43,44] It has been demonstrated that the luminescence of AuNCs was originated form the AIE of Au(I)-thiolate motifs on the NC surface.[42,45] There have also been studies on interaction between gold(I) complexes,[46,47] so we wonder if inter-NCs interaction between Au(I)-thiolate motifs on NC surface could cause the emission enhancement of the luminescent AuNCs. Herein, we studied the aggregation-induced emission enhancement (AIEE) phenomenon in AuNCs capped by glutathione.

Xie et al. have reported the AIE phenomenon of non-luminescent Au(I)-thiolate complexes,[42] as a supplementary study, in present work we studied the aggregation of luminescent clusters triggered by solvent or ions, and reported the AIEE property of GSH-AuNCs. As shown in Fig. 1A, different volumetric fractions of ethanol (f_w, vol%) were added to the GSH-AuNCs aqueous solution to investigate the luminescent intensity changes with solvent-induced aggregation. With the increasing content of ethanol, the luminescent AuNCs emits more intensively. As shown in Fig. 1B, the aggregation induced by ethanol was supported by the size analysis. The clusters formed greater aggregates with the increasing content of ethanol (0~50%), and the number of aggregates becomes more with EtOH content from 50% to 85%. When the content of ethanol was above 85%, the clusters formed denser and smaller aggregates, resulting in little decrease of the luminescent intensity. The luminescent spectra and intensity changes (Fig. 1C&D) were also in accordance with the aggregation.

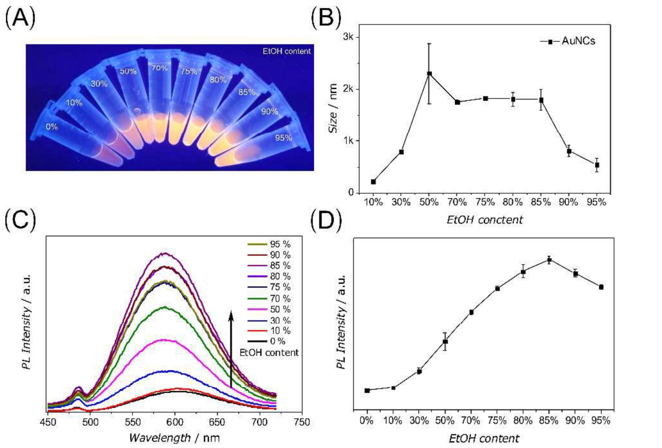

Figure 1. (A) Photographs of GSH-AuNCs in water-ethanol mixtures with different content of ethanol under UV (λ=302 nm) light. (B) Size distributions of GSH-AuNCs in water-ethanol mixtures containing different content of ethanol. (C) Photoemission spectra of GSH-AuNCs in water-ethanol mixtures containing different volume fractions of ethanol. (D) Photoemission intensity of GSH-AuNCs versus solvent composition of the water-ethanol mixture.

As depicted in Fig. 2A, since GSH form strong coordination with Pb^{2+},[48-50] that could induce the aggregation of AuNCs. We investigated the luminescent changes with the cation-induced aggregation by Pb^{2+}, as shown in Fig. 2B, the AuNCs luminesced more intensively in the presence of Pb^{2+} under UV light, indicating a cation-induced AIEE phenomenon. To further confirm that the aggregation was mediated by GSH-Pb^{2+} coordination, reversibility test was conducted by adjusting the pH of the reaction solution. As shown in Fig. 2C, there was an obvious decrease in the luminescent intensity of GSH-AuNCs when the pH of GSH-AuNCs (with Pb^{2+}) solution was adjusted to ~5.0; the luminescent intensity returned to original level after the solution pH was adjusted back to ~7.4. The isoelectric point (IP) of GSH is 5.9, and it suggested a weak interaction between divalent metal ion and amino acid under its isoelectric point due to the lack of lone pair electrons.[51] So the aggregates linked by Pb^{2+} were disassembled under GSH's IP and reassembled when pH was back to ~7.4 with corresponding decrease and increase of luminescent intensities.

The UV-vis absorption specturm of GSH-AuNCs in the absence and presence of Pb^{2+} were also recorded (Fig. 2D), adding of Pb^{2+} caused an obvious hyperchromic shift of the absorption spectrum due to the large increase in background scattering resulted from aggregates formation. The aggregation was further confirmed by TEM images of GSH-AuNCs in the absence and presence of Pb^{2+} (Fig. S1, ESI). All the results acted as certifications to demonstrate the Pb^{2+}-induced AIEE phenomenon of GSH-capped AuNCs.

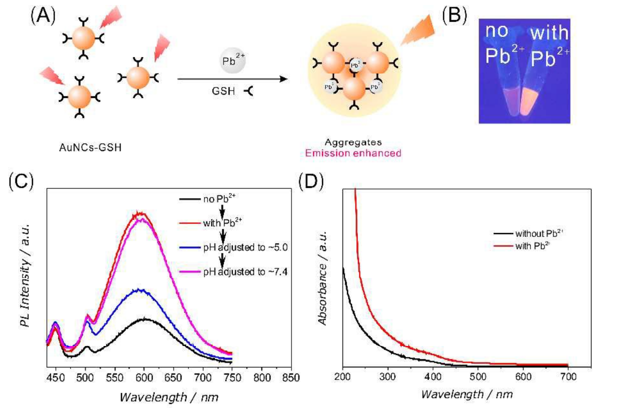

Figure 2. (A) Schematic representation of the GSH-AuNCs emission enhancement with Pb^{2+}-induced aggregation. (B) Corresponding samples under a portable UV (λ=360 nm) lamp (C) Reversibility test of Pb^{2+}-induced aggregation by adjusting the pH of aggregates solution. (D) UV−vis absorption of AuNCs in the absence and presence of Pb^{2+}.

Linear Detection of Pb^{2+}

When the GSH-AuNCs probes were mixed with Pb^{2+}, they rapidly formed bright luminescent aggregates in 1 minute (Fig. S2, ESI) through GSH-Pb^{2+}-GSH interaction and resulted in a ≈ 4-fold luminescence enhancement. The Pb^{2+}-linked aggregates exhibited photoemission peak at 590 nm when excited at 390 nm (Fig. S3, ESI), the luminescence spectra of Au-GSH NCs were collected to obtain the relationship between Pb^{2+} concentrations and luminescence intensities. As shown in Fig. 3A, the luminescence intensity increased continuously as the concentration of Pb^{2+} increased, the increases of luminescence intensity can quantitatively reflect the amount of Pb^{2+} added (Fig. 3B). A detecting linear range from 5.0 to 50 μM was obtained (R^2 = 0.99398), the lowest concentration to quantify Pb^{2+} was as low as 5 μM.

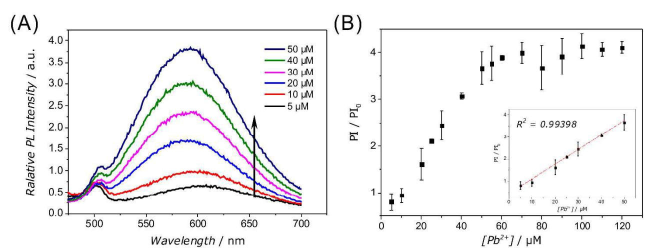

Figure 3. (A) Fluorescence spectra of AuNCs with increasing concentrations of Pb^{2+}. (B) Luminescence intensity changes at 590 nm of AuNCs as a function of the concentrations of Pb^{2+}, (inset) linear relationship in concentration range from 5.0 to 50 μM.

Selectivity

To study the selectivity of GSH-AuNCs probes, the luminescence responses were studied when the probes were challenged with other divalent metal ions (Hg^{2+}, Fe^{2+}, Pb^{2+}, Ba^{2+}, Ca^{2+}, Mn^{2+}, Zn^{2+}, Mg^{2+}, Cu^{2+}, Co^{2+}, Ni^{2+}). As shown in

Fig. 4A, in stark contrast, only the presence of Pb^{2+} brought out strong luminescence of GSH-AuNCs under UV light, negligible responses were seen from other ions at the same concentration. But the addition of some of the metal ions also caused an obvious enhancement at higher concentrations, as shown in Fig. S3-S6 in ESI, the adding of Cd^{2+} caused a ~3 fold emission enhancement of AuNCs (Cd^{2+} > 0.2 mM), there was a >70% increase when the concentration of Zn^{2+}(or Ca^{2+}) was higher than 1 mM.[46] The luminescence intensities were also recorded (Fig. 4B), 50 μM Pb^{2+} produced a higher luminescence signal compared with those caused by other metal ions (all 50 μM), showing good selectivity over all tested 12 kinds of metal ions.

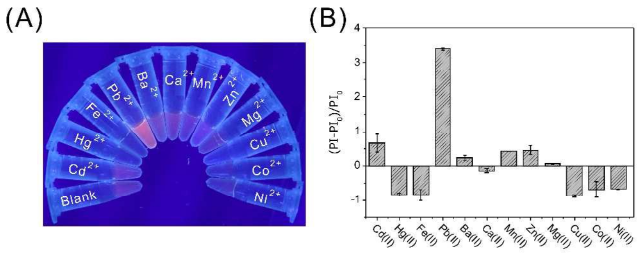

Figure 4. (A) Digital photos of GSH-AuNCs responding to 12 kinds of divalent metal ions (all 50 μM) under UV light. (B) Relative luminescence intensities at 590 nm of aqueous GSH-AuNCs solutions in the presence of different divalent metal ions.

Application

The probes' potential for real sample analysis was also evaluated by detecting Pb^{2+} in lake water. The real concentration of Pb^{2+} in lake water was firstly determined by ICP-AES, and no Pb^{2+} was detected in the samples. Then a standard addition method was used to sense Pb^{2+} ions in 10-fold diluted lake water. As shown in Fig. 5A, there was a good linear correlation between fluorescence intensities and spiked Pb^{2+} concentrations, the present approach showed its analytical efficiency in lake water sample. We also conducted an on-site testing for the contamination determination for Pb^{2+}. As shown in Fig. 5B, by using a portable UV flashlight, we could determine whether or not the water sample was contaminated with Pb^{2+}. The simple mixing-then-detection approach is simple, time-saving and economical. All these reasons led to a comprehensive result suggesting that the proposed approach has great potential for practical applications.

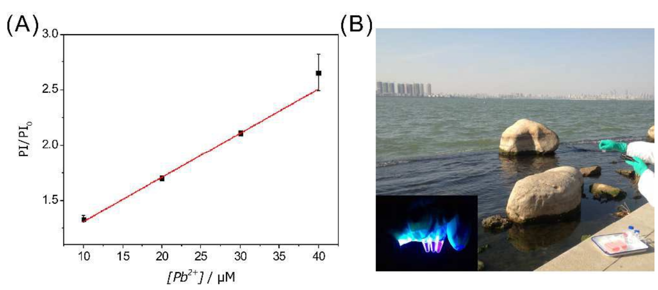

Figure 5. (A) Calibration curves of spiking concentrations of Pb^{2+} in lake water samples. (B) On-site contamination testing by using a portable LED UV (λ ≈360 nm) flashlight. Inset: Visual luminescent color changes of the GSH-AuNCs probes in different conditions (from left to right: probes only, with lake sample, with lake sample spiked with 50 μM Pb^{2+}).

Conclusions

Organic dyes or nanomaterials with interaction-responsive emission enhancement are promising luminophores for the application in analytical chemistry and biomedicine. The GSH-AuNCs was also found to have a phenomenon of aggregation-induced emission enhancement (AIEE), and the AIEE property of GSH-AuNCs has enabled us to develop a label-free turn-on method for the detection of Pb^{2+}. The method showed good linear response and selectivity, and the successful on-site detection of Pb^{2+} in real sample from lake water suggested its application potential in analytical chemistry. It is more provoking that due to the specific aurophilic Au-Au interactions between gold(I) centers, more AuNCs will be found with the AIE or AIEE phenomenon, opening up new possibilities of their synthesis and applications.

Acknowledgements

This work is supported by the National Natural Science Foundation of China (No. 21275156) and the CAS Hundred Talents program.

Notes and references

[a] College of Chemistry and Molecular Engineering, Zhengzhou University, Zhengzhou, 450001, P. R. China.
[b] Key Laboratory of Nano-Bio Interface, Division of Nanobiomedicine, Suzhou Institute of Nano-Tech and Nano-Bionics, Chinese Academy of Sciences, Suzhou, 215123, P.R. China.
[c] Key Laboratory of Analytical Chemistry for Biology and Medicine (Ministry of Education), College of Chemistry & Molecular Sciences, Wuhan University, Wuhan, 430072, P.R. China.
† The authors contributed equally to this work.
Electronic Supplementary Information (ESI) available: See DOI: 10.1039/b000000x/

1. International Lead Association (ILA) Home Page, http://www.ldaint.org/home.
2. H. Needleman, *Annu. Rev. Med.*, 2004, **55**, 209-222.
3. B. F. Reis, M. Knochen, G. Pignalosa, N. Cabrera and J. Giglio, *Talanta*, 2004, **64**, 1220-1225.
4. M. Ochsenkuhn-Petropoulou and K. M. Ochsenkuhn, *Fresenius. J. Anal. Chem.*, 2001, **369**, 629-632.
5. S. Mercan, S. Z. Ellez, Z. Turkmen, M. Yayla and S. Cengiz, *Talanta*, 2015, **132**, 222-227.
6. C. A. Mirkin, R. L. Letsinger, R. C. Mucic and J. J. Storhoff, *Nature*, 1996, **382**, 607-609.
7. Y. J. Kim, R. C. Johnson and J. T. Hupp, *Nano Lett.*, 2001, **1**, 165-167.
8. J. Liu and Y. Lu, *Nat. Protoc.*, 2006, **1**, 246-252.

9. K. Saha, S. S. Agasti, C. Kim, X. N. Li and V. M. Rotello, *Chem. Rev.*, 2012, **112**, 2739-2779.
10. R. R. Breaker and G. F. Joyce, *Chem. Biol.*, 1994, **1**, 223-229.
11. T. Lan, K. Furuya and Y. Lu, *Chem. Commun.*, 2010, **46**, 3896-3898.
12. Y. Zhao, Q. Zhang, W. Wang and Y. Jin, *Biosens. Bioelectron.*, 2013, **43**, 231-236.
13. X. H. Zhao, R. M. Kong, X. B. Zhang, H. M. Meng, W. N. Liu, W. Tan, G. L. Shen and R. Q. Yu, *Anal. Chem.*, 2011, **83**, 5062-5066.
14. Y. Lu and W. Chen, *Chem. Soc. Rev.*, 2012, **41**, 3594-3623.
15. J. Yao, M. Yang and Y. X. Duan, *Chem. Rev.*, 2014, **114**, 6130-6178.
16. Y. Y. Yang and S. W. Chen, *Nano Lett.*, 2003, **3**, 75-79.
17. R. Freeman and I. Willner, *Chem. Soc. Rev.*, 2012, **41**, 4067-4085.
18. S. Choi, R. M. Dickson and J. Yu, *Chem. Soc. Rev.*, 2012, **41**, 1867-1891.
19. Z. Luo, K. Zheng and J. Xie, *Chem. Commun.*, 2014, **50**, 5143-5155.
20. S. Y. Lim, W. Shen and Z. Gao, *Chem. Soc. Rev.*, 2015, **44**, 362-381.
21. S. Kanbak-Aksu, M. Nahid Hasan, W. R. Hagen, F. Hollmann, D. Sordi, R. A. Sheldon and I. W. Arends, *Chem. Commun.*, 2012, **48**, 5745-5747.
22. M. Lu, J. Qu, Q. Yao, C. Xu, Y. Zhan, J. Xie and J. Y. Lee, *ACS Appl. Mater. Interfaces*, 2015, **7**, 5488-5496.
23. W. Wei, Y. Lu, W. Chen and S. Chen, *J. Am. Chem. Soc.*, 2011, **133**, 2060-2063.
24. M. A. Muhammed, F. Aldeek, G. Palui, L. Trapiella-Alfonso and H. Mattoussi, *ACS nano*, 2012, **6**, 8950-8961.
25. X. Yuan, B. Zhang, Z. Luo, Q. Yao, D. T. Leong, N. Yan and J. Xie, *Angew. Chem. Int. Ed.*, 2014, **53**, 4623-4627.
26. X. D. Zhang, Z. Luo, J. Chen, X. Shen, S. Song, Y. Sun, S. Fan, F. Fan, D. T. Leong and J. Xie, *Adv Mater*, 2014, **26**, 4565-4568.
27. J. Xie, Y. Zheng and J. Y. Ying, *J. Am. Chem. Soc.*, 2009, **131**, 888-889.
28. J. Xie, Y. Zheng and J. Y. Ying, *Chem. Commun.*, 2010, **46**, 961-963.
29. C. V. Durgadas, C. P. Sharma and K. Sreenivasan, *Analyst*, 2011, **136**, 933-940.
30. D. Sen and W. Gilbert, *Nature*, 1988, **334**, 364-366.
31. Y. Guo, P. Xu, H. Hu, X. Zhou and J. Hu, *Talanta*, 2013, **114**, 138-142.
32. Y. Guo, J. Cheng, J. Wang, X. Zhou, J. Hu and R. Pei, *Chem. Asian. J.*, 2014, **9**, 2397-2401.
33. Y. Guo, L. Zhou, L. Xu, X. Zhou, J. Hu and R. Pei, *Sci. Rep.*, 2014, **4**, 7315.
34. J. Luo, Z. Xie, J. W. Lam, L. Cheng, H. Chen, C. Qiu, H. S. Kwok, X. Zhan, Y. Liu, D. Zhu and B. Z. Tang, *Chem. Commun.*, 2001, 1740-1741.
35. Y. Hong, J. W. Lam and B. Z. Tang, *Chem. Soc. Rev.*, 2011, **40**, 5361-5388.
36. Y. Okazawa, K. Kondo, M. Akita and M. Yoshizawa, *J. Am. Chem. Soc.*, 2014.
37. S. J. Ananthakrishnan, E. Varathan, E. Ravindran, N. Somanathan, V. Subramanian, A. B. Mandal, J. D. Sudha and R. Ramakrishnan, *Chem. Commun.*, 2013, **49**, 10742-10744.
38. G. Wang, R. Zhang, C. Xu, R. Zhou, J. Dong, H. Bai and X. Zhan, *ACS Appl. Mater. Interfaces*, 2014, **6**, 11136-11141.
39. K. Wang, X. Zhang, X. Zhang, B. Yang, Z. Li, Q. Zhang, Z. Huang and Y. Wei, *Colloids surf. B, Biointerfaces*, 2015, **126C**, 273-279.
40. X. Q. Cui, F. Yang, Y. F. Sha and X. R. Yang, *Talanta*, 2003, **60**, 53-61.
41. Y. Liu, Z. Wu, G. Zhou, Z. He, X. Zhou, A. Shen and J. Hu, *Chem. Commun.*, 2012, **48**, 3164-3166.
42. Z. T. Luo, X. Yuan, Y. Yu, Q. B. Zhang, D. T. Leong, J. Y. Lee and J. P. Xie, *J. Am. Chem. Soc.*, 2012, **134**, 16662-16670.
43. A. C. Dharmaratne, T. Krick and A. Dass, *J. Am. Chem. Soc.*, 2009, **131**, 13604-13605.
44. Z. Luo, V. Nachammai, B. Zhang, N. Yan, D. T. Leong, D. E. Jiang and J. Xie, *J. Am. Chem. Soc.*, 2014, **136**, 10577-10580.
45. Y. Yu, Z. Luo, D. M. Chevrier, D. T. Leong, P. Zhang, D. E. Jiang and J. Xie, *J. Am. Chem. Soc.*, 2014, **136**, 1246-1249.
46. Y. Guo, X. Tong, L. Ji, Z. Wang, H. Wang, J. Hu and R. Pei, *Chem. Commun.*, 2015, **51**, 596-598.
47. Z. Chen, J. Zhang, M. Song, J. Yin, G. A. Yu and S. H. Liu, *Chem. Commun.*, 2015, **51**, 326-329.
48. F. Chai, C. A. Wang, T. T. Wang, L. Li and Z. M. Su, *ACS Appl. Mater. Interfaces*, 2010, **2**, 1466-1470.
49. Z. Chen, H. D. Li, L. Chu, C. B. Liu and S. L. Luo, *J. Nanosci. Nanotechnol.*, 2015, **15**, 1480-1485.
50. Z. Z. Huang, H. N. Wang and W. S. Yang, *Nanoscale*, 2014, **6**, 8300-8305.
51. J. A. Dean, *Lange's Handbook of Chemistry*, 15th edn., McGraw-Hill, New York, 1999.